the nucleus may have been sufficient to cause $(\mathbf{p}_\Sigma \times \mathbf{p}_\pi)_{\text{observed}}$ to be opposite to $(\mathbf{p}_\Sigma \times \mathbf{p}_\pi)_{\text{at production}}$. This would have tended to mask any effect that might have been present.

ACKNOWLEDGMENTS

We wish to express our appreciation and indebtedness:

To Dr. Joseph J. Murray and his colleagues for providing the separated K-meson beams, and to Dr. Edward J. Lofgren and the Bevatron crew for their cooperation and aid in the exposures.

To Dr. Walter F. Dudziak, Dr. Peter C. Giles, Dr. Harry H. Heckman, and Dr. Fred W. Inman for their participation in the design and assembly of the equipment for magnetic analysis of beams, and for their help in various phases of the analyses.

To all the scanners involved in this program and particularly to Miss Ernestine Beleal, Alan Betz, Mrs. Marilyn Mollin, Mrs. Penny Vedder, and Mrs. Hester Yee for considerable assistance with the measurements and calculations.

To Mrs. Penny Vedder for much of the programming and aid with the IBM 650 computations.

To James Hodges for constructing, and participating in the design of, the automated microscopes, and to Thomas Taussig for designing the associated electronics.

PHYSICAL REVIEW VOLUME 124, NUMBER 4 NOVEMBER 15, 1961

Regeneration of Neutral K Mesons and Their Mass Difference*

R. H. Good,† R. P. Matsen,‡ F. Muller,§ O. Piccioni,‖ W. M. Powell, H. S. White, W. B. Fowler,** and R. W. Birge††
Lawrence Radiation Laboratory, University of California, Berkeley, California

(Received June 23, 1961)

A beam of K_2 mesons was produced by passing a beam of 1.1-Bev/c negative pions through a liquid hydrogen target and accepting the neutral reaction products in the forward direction after allowing the K_1 component to decay. The resultant beam was observed in a 30-in. propane bubble chamber fitted with lead and iron plates. About 200 regenerated K_1 mesons were identified by their characteristic Q value and decay rate. All three types of regeneration were observed: by transmission in the plates, by nuclear diffraction, and by interaction with single nucleons. The detection of the first two types of regeneration constitutes strong evidence for the correctness of the Gell-Mann and Pais particle mixture theory. Comparison of the transmission and diffraction regeneration effect, using the method of M. L. Good, gives the K_1-K_2 mass difference δ. Two important corrections must be applied to Good's formula: One originates from the nuclear scattering of the transmission component, the other from the multiplicity of scatterings in a thick plate. The independence from nuclear parameters, which was an advantageous property of Good's formula, is no longer rigorously valid; but due to the sharp dependence of the transmission intensity upon the mass difference, the nuclear properties of K^0 and $\bar{K}^0$, as derived from K^+ and K^- data, still allow a measurement of δ. We find that δ is $0.84_{-0.22}^{+0.29}$ in units of $\hbar/\tau_1$, where τ_1 is the K_1 mean lifetime. With 90% confidence level, the difference is between 0.44 and 1.2 $\hbar/\tau_1$. The probability that the transmission peak we observe is due to a statistical fluctuation is one in a million.

INTRODUCTION

IT is by no means certain that, if the complex ensemble of phenomena concerning the neutral K mesons were known without the benefit of the Gell-Mann–Pais theory,[1] we could, even today, correctly interpret the behavior of these particles. That their theory, published in 1955, actually preceded most of the experimental evidence known at present, is one of the most astonishing and gratifying successes in the history of the elementary particles. They advanced the hypothesis that the two mesons, K^0 and $\bar{K}^0$, are states of definite strangeness but not of definite mean life. The states which decay with a definite mean life and which, also, have a definite mass value are two other mesons, K_1 and K_2. Each of the first pair of states is a mixture of both states of the second pair, and vice versa:

$$|K^0\rangle = (|K_1\rangle + |K_2\rangle)/\sqrt{2}, \quad (1)$$

$$|\bar{K}^0\rangle = (|K_1\rangle - |K_2\rangle)/\sqrt{2}, \quad (2)$$

$$|K_1\rangle = (|K^0\rangle + |\bar{K}^0\rangle)/\sqrt{2}, \quad (3)$$

$$|K_2\rangle = (|K^0\rangle - |\bar{K}^0\rangle)/\sqrt{2}. \quad (4)$$

Only K^0 and $\bar{K}^0$ can be produced in the collisions of

* Work performed under the auspices of the U. S. Atomic Energy Commission. A preliminary report of this investigation was published by F. Muller, R. W. Birge, W. B. Fowler, R. H. Good, W. Hirsh, R. P. Matsen, L. Oswald, W. M. Powell, and H. S. White in Phys. Rev. Letters 4, 418 (1960). Parts of this research have been submitted in partial fulfillment for the degree of Doctor of Philosophy at the University of California, Berkeley, California, by R. P. Matsen and R. H. Good.

† Present address: Centre d'Etudes Nucléaires de Saclay, Gif-sur-Yvette, Seine et Oise, France.
‡ Present address: University of Wisconsin, Madison, Wisconsin.
§ Present address: Ecole Polytechnique, Paris, France.
‖ Brookhaven National Laboratory, Upton, New York. Present address: University of California at San Diego, La Jolla, California.
** Present address: Brookhaven National Laboratory, Upton, New York.
†† Present address: Ecole Polytechnique, Paris, France.

[1] M. Gell-Mann and A. Pais, Phys. Rev. 97, 1387 (1955).

strongly interacting particles because the final state must be one of a definite strangeness. However, due to the shortness (10^{-10} sec) of the K_1 mean life, the K^0 and $\bar{K}^0$ are rapidly depleted of their K_1 amplitudes, resulting in a pure state, K_2. The first confirmation of the particle-mixture theory came with the discovery of the long-lived K_2 particle by Lande *et al.*[2] Later on, several experiments were performed with the intent of showing that the K_2 particle, according to (4), contains a state $\bar{K}^0$ (strangeness -1) despite the fact that it originates from a K^0 (strangeness $+1$). The results were in satisfactory agreement with the theoretical expectations.[3,4] The most clear-cut evidence is a set of pictures by the Berkeley hydrogen bubble chamber group showing that a K^0 meson produced in association with a Λ subsequently collides with a proton and produces a Σ particle which, like the Λ, has a strangeness of -1.[5]

Encouraged by these results, one then wanted to test what has been called in the literature "even more bizarre manifestations of the mixing of K^0 and $\bar{K}^0$."[6] The point is, of course, that even though the existing evidence was in agreement with the particle mixture theory one could have possibly advanced a somewhat different explanation. In particular, it was desirable to show that the K_2 particle is composed of the two K^0 and $\bar{K}^0$ states at the same time, in the quantum-mechanical sense, rather than being a mixture of K^0 and $\bar{K}^0$ mesons in the classical sense. A most critical test of this point had been proposed.[7] If a beam of K_2 particles, perfectly parallel to each other, traverses an absorber which removes the $\bar{K}^0$ part more than the K^0, a parallel beam of K^0 will emerge from the absorber, which beam will contain a parallel beam of K_1. Such a production of one kind of particle (K_1) from a different one (K_2) with perfect conservation of the initial direction of the primary particle (which, hereafter, we will call regeneration by a plate, or by transmission) is most typical of the quantum-mechanical mixture hypothesis. One should contrast this phenomenon with, for instance, the production of neutral pions from negative pions. Obviously a parallel beam of negative pions does not produce a parallel beam of neutral pions.

It occurred to us that another test of the particle mixture theory could be made by studying the diffraction of K_2 mesons by complex nuclei. Because the K^0 and $\bar{K}^0$ part are diffracted by a nucleus with different amplitudes, the diffracted wave contains K_1 mesons. Since the angular distribution of the particles diffracted by a heavy nucleus is substantially different from the angular distribution expected for K_1 regenerated by interaction of a K_2 with a single nucleon, it is possible to decide experimentally whether the diffraction-regeneration takes place. Thus we have made an experimental study of the regeneration of K_1 from a metal plate placed in a large propane chamber. During the length of the experiment the plate was crossed by a known number of K_2 particles. All three types of regeneration have been observed: by transmission in the plate, by diffraction, and by interaction with single nucleons.

The K_1 transmission component must be thought of as generated coherently during the entire time taken by the K_2 wave to cross the plate. A mass difference of the order of 10^{-5} ev between these two particles makes the phase difference between the two states change as the wave goes through the plate, a phenomenon similar to the one that leads to the oscillation between the states K^0 and $\bar{K}^0$, noticed by Serber.[8] The effect of the mass difference on the intensity of the transmission component was first studied by Case,[9] but it was after the treatment by M. L. Good[10] that one could think of using the effect for measuring the mass difference. From our work the difference appears to be $(5.5\pm1.7)\times10^{-6}$ ev, that is, $(0.84\pm0.25)\hbar/\tau_1$, where τ_1 is the mean life of K_1.

On the subject of the mass difference, one pioneering work had been done before our experiment,[11] with a result in qualitative agreement with the particle mixture theory for a mass difference of the order of magnitude of $\hbar/\tau_1$. Subsequent to our work, Birge *et al.*[12] undertook a measurement of the mass difference, based on an accurate study of the Serber effect. Their preliminary report at the Rochester Conference shows a value of $(1.5\pm0.5)\hbar/\tau_1$, in fairly good agreement with ours.

SECTION I

Regeneration by Nucleons, by Nuclei, and by the Plate

Assuming that the four heavy mesons belong to two isotopic doublets, K^+ and K^0, K^- and $\bar{K}^0$, all the three types of regeneration can be quantitatively estimated from the scattering properties of charged K's interacting on nucleons or on nuclei. We represent the incoming

[2] K. Lande, L. M. Lederman, and W. Chinowsky, Phys. Rev. **105**, 1925 (1957).
[3] R. Ammar, J. I. Friedman, R. Levi Setti, and L. I. Telegdi, Nuovo cimento **5**, 1801 (1957); M. Baldo-Ceolin, C. C. Dilworth, W. F. Fry, W. D. B. Greening, H. Huzita, S. Limentani, and A. E. Sicherollo, *ibid.* **6**, 130 (1957); M. Baldo-Ceolin, N. Huzita, S. Natali, U. Camerini, and W. F. Fry, Phys. Rev. **112**, 2118 (1958); V. Bisi, R. Cester, A. Debenedetti, C. M. Garelli, N. Margem, B. Quassiati, and M. Vigone, Nuovo cimento **12**, 16 (1959).
[4] W. B. Fowler, R. L. Lander, and W. M. Powell, Phys. Rev. **113**, 928 (1959).
[5] F. S. Crawford, Jr., M. Cresti, M. L. Good, K. Gottstein, E. M. Lyman, F. T. Solmitz, M. L. Stevenson, and H. Ticho, Phys. Rev. **113**, 1601 (1959).
[6] J. D. Jackson, *The Physics of Elementary Particles* (Princeton University Press, Princeton, New Jersey, 1958), p. 75.
[7] A. Pais and O. Piccioni, Phys. Rev. **100**, 1487 (1955).
[8] R. Serber, quoted in reference 7. See also W. F. Fry and R. G. Sachs of Phys. Rev. **109**, 2212 (1958).
[9] K. M. Case, Phys. Rev. **103**, 1449 (1956).
[10] M. L. Good, Phys. Rev. **106**, 591 (1957); **110**, 550 (1958).
[11] E. Boldt, D. O. Caldwell, and Y. Pal, Phys. Rev. Letters **1**, 150 (1958).
[12] R. W. Birge, R. P. Ely, W. M. Powell, H. Huzita, W. F. Fry, J. A. Gaides, S. Natali, R. B. Willman, and U. Camerini, *Proceedings of the 1960 International Conference on High-Energy Physics at Rochester* (Interscience Publishers, Inc., New York, 1960), p. 601.

K_2 wave as

$$|K_2\rangle=(|K^0\rangle-|\bar{K}^0\rangle)/\sqrt{2}. \quad (4)$$

This representation is slightly incorrect if invariance with respect to the combined operation of charge and space inversion (PC) is not rigorously respected by the weak interactions. Lee *et al.*[13] have treated this subject with the less restrictive assumption of invariance with respect to PCT, showing that, in general, the coefficients of K^0 and $\bar{K}^0$ in the formula (4) are not necessarily $1/\sqrt{2}$ and $-1/\sqrt{2}$. However, the same authors and also Weinberg[14] have shown that, due to the large disparity between the mean lives of K_2 and K_1, the coefficients in question must be almost equal. We thus put them equal for simplicity as this has practically no effect on our results.

When the K_2 wave hits a target, the scattered wave will be the state given by

$$(f_+|K^0\rangle-f_-|\bar{K}^0\rangle)/\sqrt{2},$$

which can also be expressed as

$$[(f_+-f_-)/\sqrt{2}]|K_1\rangle+[(f_++f_-)/\sqrt{2}]|K_2\rangle,$$

in terms of a regenerated amplitude and a scattered amplitude.

A. Regeneration by Nucleons

When a K_2 collides with a nucleus, we must distinguish the two cases according to whether the nucleus is left in its initial state, or in a different state, most probably consisting of a different nucleus and one or more secondary nucleons. In the first case we have elastic nuclear regeneration, produced by the nucleus as a whole (see Sec. I.B), but in the second case, we have inelastic nuclear regeneration that can only be thought of as regeneration originated by one or more collisions of the K_2 with the individual nucleons in the nucleus. While we do not have enough information to compute the total cross section for the inelastic regeneration, we want nevertheless to show that the differential cross section for inelastic regeneration is, at small angles, much smaller than for the elastic regeneration, treated in Sec. I.B.

The four scattering amplitudes (K^+,n), (K^+,p), (K^-,n), and (K^-,p) which we need in order to compute f_+ and f_- for the nucleonic regeneration are not well known at the present time, but one can make an approximate estimate of the forward differential scattering by computing the imaginary part of such amplitudes, which are directly related to the total cross section by the optical theorem. At our energy, the total cross section of K^+ proton is 15 mb and the total cross section of K^+ neutron appears to be substantially the same. The total cross section of K^- proton is about 40 mb while the total cross section of K^- neutron is 28 mb.[15] With obvious notations we have

$$\mathrm{Im}(f_+^0-f_-^0)/2=(\sigma^+-\sigma^-)/8\pi\lambda=\mathrm{Im}f_{21}^0,$$

which gives the imaginary part of the amplitude in the forward direction for production of K_1 mesons from K_2 in collisions with individual nucleons. For collisions of K_2's with protons, σ^- and σ^+ are, respectively, the total cross sections of K^- on neutrons and K^+ on neutrons, while for collisions of K_2 with neutrons σ^- and σ^+ must be taken equal to the values of the total cross sections with protons. Substituting the numbers, we have that the square of the imaginary part of f_{21}^0 gives one millibarn per steradian as forward differential cross section for regeneration for the case of K_2 particles impinging on neutrons and 0.28 millibarn per steradian for K_2's impinging on protons.

As the nucleus of iron contains 26 protons and 30 neutrons, we have a total of 37 mb/sr for the regeneration of K_1 by collisions of K_2's with the single nucleons in the iron nucleus. This is, of course, only the contribution of the imaginary part to the differential cross section. The inclusion of the real part would increase these three numbers, though not by a large factor. On the other hand, one must bear in mind that there is a shadow effect; some of the nucleons in the nucleus only receive an attenuated K_2 beam. In addition to this, the forward cross section is strongly limited by the fact that the Pauli principle forbids regeneration collisions with small momentum transfers to the nucleon. The inelastic regeneration by the nucleus is therefore negligible at small angles compared to 280 mb/sr which we compute, in the next section, for the coherent, or elastic, diffraction type regeneration.

B. Diffraction Regeneration by Nuclei

For the regeneration that takes place from a nucleus as a whole, that is when the nucleus after the collision is left in the same state as it was, we need the scattering amplitude f_+ and f_- to be taken as those of K's on nuclei, and we compute them by the optical model method.[16] To an approximation which is acceptable in our case a complex nucleus such as iron can be considered as containing as many neutrons as protons; therefore, the scattering amplitude for K^0 (and $\bar{K}^0$) can be taken as equal to that of K^+ (K^-). First we consider the case of the K^0 for which there is a potential $V(r)$ inside the iron nucleus. The relativistic energy relation for the K^0 while it is inside the nucleus is given by

$$(E_0-V)^2=(pc)^2+(m_Kc^2)^2,$$

[13] T. D. Lee, R. Oehme, and C. N. Yang, Phys. Rev. **106**, 340 (1957). K. Aizu, Nuovo cimento **6**, 1040 (1957).

[14] S. Weinberg, Phys. Rev. **110**, 782 (1957).

[15] O. Chamberlain, L. M. Crowe, D. Keefe, L. T. Kerth, A. Lemonick, T. Maung, and T. F. Zipf (to be published); H. C. Burrowes, D. O. Caldwell, D. H. Frisch, D. A. Hill, D. M. Ritson, and R. A. Schluter, Phys. Rev. Letters **2**, 117 (1959); See also report by L. W. Alvarez, at the *Ninth Annual International Conference on High-Energy Physics, Kiev, 1959* (Academy of Science, U.S.S.R., 1960).

[16] S. Fernbach, R. Serber, and T. B. Taylor, Phys. Rev. **75**, 1352 (1949).

TABLE I. Nuclear cross sections, computed according to various optical model parameters, for iron. $p=670$ Mev/c; $V=\mathrm{Re}K^+$ pot. $=1.35$ Mev; $W=\mathrm{Im}K^+$ pot. $=-17.6$ Mev. $|N\Lambda\lambda f_{21}{}^0|^2$ is proportional to the transmission intensity.

	Real K^- pot. (Mev)	σ_{K^-} (mb)	σ_{21} (mb)	σ_{22} (mb)	σ_{in} (mb)	σ_T (mb)	$\lvert N\Lambda\lambda f_{21}{}^0\rvert^2$
Set No. 1	0	33.2	12.4	281	584	865	1.08×10^{-3}
Set No. 2	−15	33.2	25.8	289	597	886	2.31×10^{-3}
Set No. 3	0	25	8.64	242	551	793	0.74×10^{-3}
Set No. 4	0	40	16.0	303	603	906	1.41×10^{-3}
Set No. 5	0	55	24.9	341	638	979	2.24×10^{-3}

and outside the nucleus it is given by

$$E_0{}^2=(p_0c)^2+(m_Kc^2)^2,$$

so that in the approximation that V is much less than E_0 we have

$$p-p_0=\Delta p=(-E_0/p_0c^2)V,$$
$$\Delta k=-(E_0/\hbar p_0c^2)V.$$

After the K meson has traveled a distance l through the nucleus, its amplitude is $\eta_+\exp(ik_0l)$, where

$$\eta_+=\exp\left(i\int_0^l\Delta k dx\right),$$

and the amplitude for elastic K^0 scattering from the entire nucleus is given by

$$f_+(\theta)=ik_0\int_0^R(1-\eta_+)J_0(k_0\rho\sin\theta)\rho d\rho. \tag{5}$$

ρ is the distance between the center of the nucleus and the meson trajectory, so that l and η are functions of ρ.

In accordance with the principle of charge independence we take the K^0 potential to be equal to the K^+ potential which has been measured in emulsion by Sechi-Zorn and Zorn.[17] They fit their data to a Woods-Saxon potential[18] of the type given by

$$V(r)=(V+iW)\Big/\left[1+\exp\left(\frac{r-r_0}{d}\right)\right],$$

where

$$r_0=1.15A^{\frac{1}{3}}\times10^{-13}\text{ cm},$$

and

$$d=0.57\times10^{-13}\text{ cm}.$$

The values of V and W are found in Tables I and II.

In the same way, f_- is obtained when the $\bar{K}^0$ potential is replaced by the highly absorptive K^- potential. In the absence of experimental information on the K^- nuclear potential, we assume that it is entirely absorptive and is determined by the K^--nucleon total cross section. We then have

$$f_-(\theta)=ik_0\int_0^R(1-\eta_-)J_0(k_0\rho\sin\theta)\rho d\rho,$$
$$\eta_-=\exp\left(-\frac{\sigma^-D_0}{2}\right)\int_0^l\frac{dx}{1+\exp[(r-r_0)/d]}, \tag{6}$$

where σ^- is the total cross section of K^- averaged with respect to neutrons and protons and D_0 is the density of nucleons at the center of the iron nucleus ($0.135\times10^{+39}$ nucleons per cubic cm). At present the best value for σ^- appears to be 33 mb.[15] Figure 1 gives the scattering amplitude $f_{22}=f_{11}=(f_++f_-)/2$ and the regeneration amplitude $f_{12}=f_{21}=(f_+-f_-)/2$ for the momentum of 670 Mev/c and for a purely imaginary potential for K^-. Figure 2 gives the corresponding differential cross sections. The integrated cross sections can be obtained by numerically integrating the curves of Fig. 2 or they can be computed from the relations:

$$\sigma_{21}=2\pi\int_0^R\left|\frac{\eta_+-\eta_-}{2}\right|^2\rho d\rho, \tag{7}$$

$$\sigma_{22\mathrm{el}}=2\pi\int_0^R\left|\frac{2-\eta_+-\eta_-}{2}\right|^2\rho d\rho, \tag{8}$$

$$\sigma_{22\mathrm{in}}=2\pi\int_0^R\left[1-\left|\frac{\eta_++\eta_-}{2}\right|^2\right]\rho d\rho. \tag{9}$$

TABLE II. Nuclear cross sections, computed according to various optical model parameters, for iron, for different values of the K_2 momentum. Real K^- pot. $=0$; $\sigma_{K^-}=38.2$ mb. $|N\Lambda\lambda f_{21}{}^0|^2$ is proportional to the transmission intensity.

	p (Mev/c)	$V=\mathrm{Re}K^+$ pot. (Mev)	$W=\mathrm{Im}K^+$ pot. (Mev)	σ_{21} (mb)	σ_{22} (mb)	σ_{in} (mb)	σ_T (mb)	$\lvert N\Lambda\lambda f_{21}{}^0\rvert^2$
Set No. 1A	565	18.5	−17.4	16.3	311	588	899	0.96×10^{-3}
Set No. 1	670	13.5	−17.6	12.4	281	584	865	1.08×10^{-3}
Set No. 1B	775	13.5	−17.6	14.9	272	570	842	1.73×10^{-3}

[17] B. Sechi-Zorn and G. T. Zorn, Phys. Rev. **120**, 1898 (1960).
[18] R. D. Woods and D. S. Saxon, Phys. Rev. **95**, 577 (1954).

C. *Transmission Regeneration by a Plate*

When a K_2 beam crosses a plate, we have not only the nucleonic (inelastic) and nuclear (elastic) regeneration from the nuclei in the plate, but also the coherent action of all the nuclei producing a parallel beam of regenerated K_1 in the forward direction. That this happens is most evident if one considers the idealized case treated in reference 7. If the plate is completely opaque to $\bar{K}^0$ particles and completely transparent to K^0 particles, the K^0 wave, contained in the K_2 beam, proceeds undisturbed after crossing the plate and, of course, will constitute a parallel beam of K^0 which in turn contains a parallel beam of K_1's. M. L. Good[10] has shown that a parallel beam of regenerated K_1's appears not only in the idealized case of reference 7 but, in general, whenever the interaction of $\bar{K}^0$ with nuclei is different from the interaction of the K^0 particles.

We follow here a somewhat different method of analysis than the one used by M. L. Good. The K_2 wave, $a_2(x)|K_2\rangle$, passing through the plate, causes each thickness dx of the plate to emit a plane wave:

$$[i\lambda N a_2(x)/\sqrt{2}][f_+{}^0|K^0\rangle - f_-{}^0|\bar{K}^0\rangle]dx,$$

which contains the wave:

$$\tfrac{1}{2}i\lambda N a_2(x)(f_+{}^0 - f_-{}^0)|K_1\rangle dx. \tag{10}$$

The superscripts on the f's indicate that these are the nuclear scattering amplitudes in the forward direction. This is quite similar to computing the attenuation in amplitude of a beam of, say, protons passing through the plate of thickness dx. The plate emits in the forward direction a wave of amplitude $da = ia\lambda N f^0 dx$, where a is the incoming wave of protons, f^0 is the amplitude for forward elastic scattering by the nuclei, and N is the number of nuclei per cubic centimeter. The fractional decrease of the wave amplitude is $N\lambda\,\mathrm{Im}f^0 dx$, which, because of the optical theorem relation $\sigma_T = 4\pi\lambda\,\mathrm{Im}f^0$, is equal to $N\sigma_T dx/2$, which shows an intensity attenuation equal to $N\sigma_T dx$.

The particle picture would obviously and quickly give the same result. This kind of reasoning would be wrong if applied to the passage of light through a condensed medium such as water, for it is known that the field acting on each scattering center in that case is different from the free field of the electromagnetic wave. The forward wave resulting from the radiation from all scattering centers is then $da = ia\lambda N c f^0 dx$, where c is the ratio of the effective field to the wave field,[19] and is equal to $1+(4\pi P)/3E$, where P is the polarization of the medium and E is electrical field. Clearly, in our case no such correction is needed; otherwise we should doubt the method of obtaining the proton-nucleus total cross section by measuring the absorption of a proton beam passing through a plate. Note that in the idealized case of reference 7, the production of a K_1 plane wave is directly related to the difference in the *absorption* of the K^0 and $\bar{K}^0$ waves.

[19] M. Lax, Revs. Modern Phys. **23**, 287 (1951).

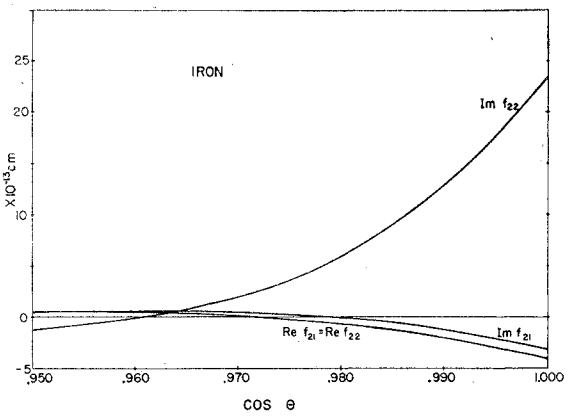

FIG. 1. The scattering amplitudes f_{21} and f_{22} as calculated according to the optical model for the nuclear parameters labeled as Set No. 1 in Table I.

Our procedure can be greatly simplified by making use of the fact, pointed out by M. L. Good, that the total intensity of the regenerated K_1's never exceeds one percent of the K_2 intensity, so that the regeneration of K_2's by the regenerated K_1's can be neglected. We then just compute the K_1 amplitude produced at each depth in the plate, take into account its attenuation because of absorption and decay before reaching the end of the plate, and add the amplitudes at all depths in the plate. These amplitudes add coherently with each other, because of the basic fact that each nucleus remains in the same state after the production of K_1 as it was before. Now the momentum k_1 of the regenerated K_1 is different from k_2, the momentum of K_2, because of the difference in mass between the two particles. Therefore a difference in phase between amplitudes produced at two different

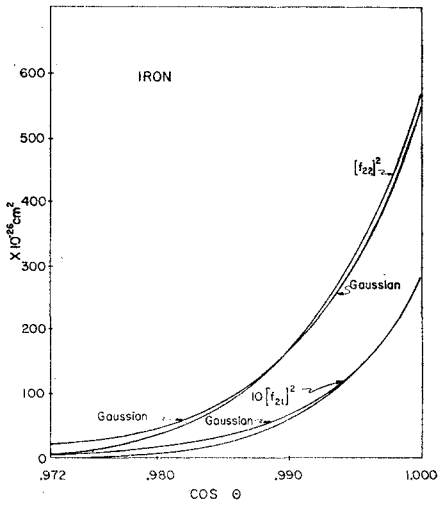

FIG. 2. The differential cross sections for diffraction regeneration and for diffraction scattering, with corresponding Gaussian approximations, computed from the amplitudes of Fig. 1.

depths is introduced by the fact that while both waves obviously cross the same thickness, the fraction of such path during which the wave is K_1 is different. It is fortunate that, as remarked by Good, the absorption mean free path of K_1 is the same as that of K_2 (because for either particle the absorption cross section is the average of the cross section for K^0 and $\bar{K}^0$), so that we can compute our relevant quantities without knowing it. The "absorption" by decay is different for K_1 and K_2, and is only important for K_1, the lifetime of which is sufficiently well known.

The amplitude of K_1 produced in the thickness dx at the depth x is then

$$iN\lambda f_{21}{}^0 \exp(ik_2x)dx,$$

and will arrive at the end of the plate ($x=L$) with the amplitude $d\alpha_1$:

$$d\alpha_1=iN\lambda f_{21}{}^0 \exp[ik_2x+ik_1(L-x) -(L-x)/2v\gamma\tau_1-NL\sigma_T/2]dx, \quad (11)$$

where σ_T is the total cross section for K_1 and K_2, v is the velocity of the particles, γ is the Lorentz factor, and k_1 and k_2 are the momenta of the K_1 and K_2.

In elastic nuclear collisions resulting in the transformation of K_2 into K_1 the momentum of the emerging K_1 will differ by a small amount Δk from the initial momentum of the impinging K_2. If $\Delta k=k_1-k_2$, the nucleus will recoil with the momentum $-\Delta k$, subtracting from the meson the energy $(\Delta k)^2/2M$, where M is the mass of the nucleus. This energy is negligible with respect to the mass difference. Thus Δk can be computed assuming that K_1 has the same total energy as K_2, that is,

$$\Delta k=k_1-k_2=\frac{-mc^2}{(\hbar c)^2k}(m_1-m_2)c^2,$$

where m and k can be taken as the mass and momentum of either meson.

It may be noticed that we use here one definite value for the mass difference between K_1 and K_2. Actually, the mass spectrum for both mesons has a finite width as a consequence of their finite lifetimes. In particular, the spread $(\hbar/\tau_1)$ of the mass values for K_1 is larger than the mass difference between K_1 and K_2 deduced from the results of this experiment. The point to be emphasized is that when we write for the wave generated in the thickness dx the expression $\exp(-im_1t/\hbar)\exp(-t/2\tau_1)$ or the corresponding $\exp(ik_1x)\exp(-x/2\gamma v\tau_1)$, we imply already the production of a spectrum of masses, with a central value of m_1 and a width given by the spread of the Fourier spectrum, namely $\hbar/\tau_1$, as it should be.

If we call $\Lambda=\gamma v\tau_1$ the decay mean free path of the K_1 and introduce the dimensionless quantities $l=L/\Lambda$ and $\delta=(m_2-m_1)c^2/(\hbar/\tau_1)$, we obtain from (11):

$$|\alpha(l)|^2=\frac{|f_{21}{}^0|^2(N\lambda\Lambda)^2}{\delta^2+\frac{1}{4}}|e^{-i\delta l}-e^{-l/2}|^2e^{-NL\sigma_T}. \quad (12)$$

This is therefore the intensity of the undeflected wave of regenerated K_1's already obtained by M. L. Good by a somewhat different procedure.

SECTION II

Multiple Scattering

If we could ignore some inherent complications, we would quickly compute the intensity of K_1's regenerated from the nuclei by the diffraction process. The production per unit solid angle in the forward direction would be

$$(dn_1/d\Omega)^0=|f_{21}{}^0|^2N\Lambda(1-e^{-l})e^{-NL\sigma_T}, \quad (13)$$

with the interesting property that the ratio of (12) to (13) is independent of the actual value of $f_{21}{}^0$, so that the measurement of that ratio would allow us to derive the mass difference in terms of the other known parameters appearing in (12) and (13), without knowing $f_{21}{}^0$. Actually, the situation is not quite so favorable. First, we must take into account that the K_2 wave, $a_2|K_2\rangle$, proceeding through the plate until it hits a nucleus, has already accumulated a K_1 amplitude by the process of transmission regeneration represented by formula (10), and during the rest of the path, after the nuclear collision until reaching the end of the plate, again a K_1 amplitude is accumulated by process (10).

Secondly, in a 15-cm plate, the probability that the wave undergoes only one collision is comparable with the probability of undergoing more than one collision, and we must therefore take into account this multiple scattering and regeneration mechanism. The independence from f_{22} and f_{21} is no longer with us, but the intensity (12) depends so critically on the mass difference that we can still obtain its value from the present experiment and an approximate knowledge of f_{22} and f_{21}.

It pays to reproduce the analysis in some detail. We want to find the amplitude of the K_1 wave emerging from the plate, after undergoing 0, 1, $\cdots$, n collisions, respectively. Note that each collision can occur at any depth and can produce any (small) scattering angle, with or without regeneration. Waves corresponding to different collision-depths or to different angles in each collision (even if they have the same final angle at the end of the plate) are incoherent with each other, and must be added in intensity, not in amplitude.

The wave emerging from the plate without nuclear encounters is that which we have called the transmission-regenerated wave. Its amplitude is

$$\alpha(l)=iN\lambda\Lambda f_{21}{}^0(e^{-i\delta l}-e^{-l/2}) \times(-i\delta+\tfrac{1}{2})^{-1}e^{-NL\sigma_T/2}e^{ik_1L}. \quad (14)$$

The wave emerging from the plate after one collision at a depth x will have an amplitude depending upon the scattering angle θ. This wave, as we have already mentioned, arises from two processes:

(i) Ordinary scattering. The transmission wave accumulated between 0 and x is ordinarily diffracted and reaches the end of the plate with the amplitude:

$$\left\{iN\lambda f_{21}^0\int_0^x e^{ik_2y}\exp[(ik_1-1/2\Lambda)(x-y)]dy\right\}$$
$$\times f_{22}(\theta)\exp[(ik_1-1/2\Lambda)(L-x)]e^{-NL\sigma T/2}. \quad (15)$$

At the same time the K_2 wave is ordinarily diffracted at the depth x, in the direction θ, and produces, in the path from x to the end of the plate, the transmission-regenerated K_1 wave:

$$f_{22}(\theta)\left\{iN\lambda f_{21}^0\int_x^L e^{ik_2y}\right.$$
$$\left.\times\exp[(ik_1-1/2\Lambda)(L-y)]dy\right\}e^{-NL\sigma T/2}. \quad (16)$$

The two amplitudes (15) and (16) must be added, obtaining $\alpha(l)f_{22}(\theta)$, that is, the no-collision transmission wave (14) multiplied by $f_{22}^0(\theta)$. Note that this amplitude is independent of x. This feature, which remains true for n scatterings, hinges on the fact that both K_1 and K_2 scatter with identical amplitudes, so that the accumulation of the transmission wave, which can be thought of as due to a large number of collisions at a large distance, continues in the new direction of motion just as it would have continued in the initial direction. Thus the depth at which the scattering takes place is of no importance.

(ii) Regenerative diffraction of the K_2 wave at x, which results in the amplitude $\eta(x)f_{21}(\theta)$, where

$$\eta(x)=e^{(-i\Delta k+1/2\Lambda)x}e^{-l/2}e^{ik_1L}e^{-NL\sigma T/2}$$
$$=e^{(-i\delta+\frac{1}{2})x/\Lambda}e^{-l/2}e^{ik_1L}e^{-NL\sigma T/2}. \quad (17)$$

In the case of n collisions, regeneration of K_1 from K_2 can occur at any of the collisions. We can neglect regeneration of K_2 from K_1, in view of the much larger amplitude of K_2 with respect to K_1 at any depth. We must follow the accumulated transmission-regenerated K_1 wave in its scattering at all points. Its amplitude is

$$\alpha(l)f_{22}(\theta_1)f_{22}(\theta_2)\cdots f_{22}(\theta_n). \quad (18)$$

The whole K_1 amplitude due to n scatterings on n nuclei at $x_1, x_2, \cdots, x_n$, respectively, is

$$\eta(x_1)f_{21}(\theta_1)f_{22}(\theta_2)f_{22}(\theta_3)\cdots f_{22}(\theta_n)$$
$$+\eta(x_2)f_{22}(\theta_1)f_{21}(\theta_2)f_{22}(\theta_3)\cdots f_{22}(\theta_n)+\cdots$$
$$+\eta(x_n)f_{22}(\theta_1)f_{22}(\theta_2)f_{22}(\theta_3)\cdots f_{21}(\theta_n)$$
$$+\alpha(l)f_{22}(\theta_1)f_{22}(\theta_2)\cdots f_{22}(\theta_n). \quad (19)$$

From inspection of the computed amplitudes f_{21} and f_{22} we conclude that for the purpose of computing the contribution of multiple scattering processes, and the broadening of the angular distribution caused by multiple collisions, we can make the approximation $f_{21}(\theta)/f_{22}(\theta)=f_{21}^0/f_{22}^0$. (We have also made a more laborious computation without this approximation. The angular distribution as well as the predicted intensity do not change appreciably.) Formula (19) can thus be written:

$$F_n=\left[\frac{f_{21}^0}{f_{22}^0}\sum_{i=0}^{n}\eta(x_i)+\alpha(l)\right]f_{22}(\theta_1)\cdots f_{22}(\theta_n). \quad (20)$$

In order to find the number of K_1's at an angle θ as a result of n collisions we have to form the square of the absolute value of F_n, integrate over all angles θ_i bound by the condition that the total deflection be θ, then multiply by $N^n dx_1\cdots dx_n$ and integrate over all x_i. The integration over the angles, that is, the folding together of n angular distribution such as these, can be expected to be a tedious problem. However, in this case, where the angular distributions have a diffraction shape, and for the small angles of our problem, each distribution may be closely approximated (see Fig. 2) by a Gaussian distribution:

$$|f_{22}(\theta)|^2\approx|f_{22}^0|^2\exp(-\theta^2/2b^2)$$
$$=|f_{22}^0|^2\exp[-(1-\cos\theta)/b^2]. \quad (21)$$

Since the result of folding two Gaussian distributions (for small angles) is still a Gaussian, our problem of combining angular distributions is simplified. Furthermore, any number of scatterings may be treated by making repetitive use of this law of combination. The law of combination for the n Gaussian distributions $|f_{22}^0|^2\exp(-\theta_i^2/2b^2)$ is

$$\int\prod_{i=1}^{n}|f_{22}^0|^2\exp\left(\frac{-\theta_i^2}{2b^2}\right)d\Omega_1\cdots d\Omega_n$$
$$=\frac{(2\pi b^2|f_{22}^0|^2)^n}{2\pi}\frac{1}{nb^2}\exp\left(\frac{-\theta^2}{2nb^2}\right),$$

with the approximation on the solid angles that $d\Omega=\theta d\theta d\phi$; the integration on the left-hand side is taken over angles θ_i such that the resultant angle with the initial direction is θ. Using the same approximation, we have

$$\sigma_{22}=2\pi|f_{22}^0|^2b^2;$$

the n folded Gaussians yield

$$\sigma_{22}{}^nG_n(\theta),$$

where $G_n(\theta)=(1/2\pi nb^2)\exp(-\theta^2/2nb^2)$. ($G_n$ is a normalized Gaussian.) Thus the integrated cross section for the n folded Gaussians is the product of the cross sections for each Gaussian, as it should be.

Multiplying (20) by its complex conjugate and integrating with respect to the angles $\theta_1, \cdots, \theta_n$, we have

$$\left|\frac{f_{21}^0}{f_{22}^0}\sum_{i=0}^{n}\eta(x_i)+\alpha(l)\right|^2\sigma_{22}{}^nG_n(\theta). \tag{22}$$

Formula (22) represents the probability for a collision with a nucleus at x_1, another at x_2, and so on. We need the probability for such collisions to occur, within each dx; then we must integrate over all possible depths, as well as sum over all possible numbers of collisions. Thus we must multiply (22) by $N^n dx_1 dx_2 \cdots dx_n$ and integrate. If we introduce the abbreviation:

$$\varphi(l,\delta)=|e^{-i\delta l}-e^{-l/2}|^2/(\delta^2+\tfrac{1}{4}),$$

we then have

$$I(\theta)=\sum_{n=1}^{\infty}I_n(\theta)=\sum_{n=1}^{\infty}e^{-NL\sigma_T}\frac{(NL\sigma_{22})^nG_n(\theta)}{n!}|f_{21}^0|^2$$
$$\times\left\{\frac{n(1-e^{-l})}{l|f_{22}^0|^2}+(N\lambda\Lambda)^2\varphi+\frac{n(n-1)}{l^2|f_{22}^0|^2}\varphi\right.$$
$$\left.-\frac{nN\Lambda\sigma_T}{l|f_{22}^0|^2}\right\}\varphi, \tag{23}$$

where

$$L=l\Lambda;\quad \sigma_T=4\pi\lambda\,\mathrm{Im}f_{22}^0.$$

The first term in the bracket arises from regeneration in a single scattering process; the second is the scattered transmission regeneration; the third is due to the interference of the scattered-regenerated K_1 waves from the n nuclei with each other, and the fourth is due to interference between transmission-regenerated and collision-regenerated K_1 waves. In practice the entire expression becomes negligible for $n>4$ scatterings. $I(\theta)$ is the number of K_1's regenerated in one or more nuclear collisions, per unit solid angle and per one K_2 arriving on the plate. The transmission component, that is the number of K_1's (all in the forward direction) regenerated per one incident K_2, has already been given (12) and can be rewritten:

$$I_T=(N\lambda\Lambda)^2|f_{21}^0|^2e^{-NL\sigma_T}\varphi. \tag{24}$$

The necessity of using the multiple scattering formula (23) is illustrated by the values of the probabilities that the neutral meson, either in K_1 or K_2 state, undergoes respectively 0, 1, 2, 3 elastic collisions in the 6-in. plate without suffering inelastic encounters. Using the nuclear parameters of Set No. 1 of Table I we find, respectively, 0.33; 0.119; 0.021; 0.003. The relative numbers of K_1's produced by K_2's in traversals with 0, 1, 2, 3, collisions are, for $\delta=0.8\hbar/\tau_1$, respectively, 0.257; 0.467; 0.214; 0.055, with the property that the 0.257 K_1's are all produced forward.

Formulas (24) and (23) may be compared with M. L. Good's elegant expression for the ratio R of transmission-regenerated K_1's (integrated with respect to the solid angle) to diffraction-regenerated K_1's (per unit solid angle) in the forward direction. In the above notation, his formula is

$$R=N\Lambda\lambda^2\varphi/(1-e^{-l}). \tag{25}$$

Corresponding to this we have the ratio of (24) to the $n=1$ term of (23) (single scattering regeneration).

$$R=\frac{N\Lambda\lambda^2\varphi}{1-e^{-l}+(N\Lambda\lambda)^2l|f_{22}^0|^2\varphi-N\Lambda\sigma_T\varphi}. \tag{26}$$

This reduces to Good's formula if transmission regeneration along the path of scattered K_2's is neglected (last two terms in denominator).

Taking also into account the multiple scattering, we have

$$R=I_T/I(\theta), \tag{27}$$

where I_T and $I(\theta)$ are given by (23) and (24). The values of R according to the three different expressions (25), (26), and (27), are, respectively, 0.0365, 0.0844, and 0.0548 for $\delta=0$ and 0.0177, 0.0255, and 0.0202 for $\delta=0.8$.

The corrections to the formula of Good have an appreciable effect on the computed value of R. They also destroy the attractive feature in Good's formula that R is independent of the nuclear parameters like f_{21}, f_{22}, σ_T, σ_{22}. We have thus asked ourselves whether the determination of δ is still possible from formula (27) which requires the knowledge of nuclear parameters whose values have not been experimentally measured. The answer is in the affirmative, because any reasonable set of values substituted in (27) yields substantially the same result. First of all, we have already seen that the dependence on σ_{21} and f_{21} (which are the most

TABLE III. Values of R=transmission peak/diffraction regeneration for several choices of the elastic scattering cross section σ_{22} and the mass difference δ.

σ_{22} \ δ	0	0.4	0.8	1.2	1.6
281 mb	0.055	0.041	0.0202	0.0078	0.0033
140 mb	0.052	0.04	0.0195	0.0075	0.0028
562 mb	0.047	0.035	0.0165	0.0062	0.0023

TABLE IV. Regeneration (σ_{21}), elastic (σ_{22}), and inelastic (σ_{in}) cross sections for three nuclei. b^2 gives the width of the angular distribution for the processes of elastic scattering and regeneration (see text). The three last rows refer to the amplitudes.

	Carbon	Iron	Lead
σ_{21} (mb)	8.3	25.8	41.6
σ_{22} (mb)	51.3	289	996
σ_{in} (mb)	177	597	1510
b^2 (rad)^2	0.0214	0.00784	0.00364
$\lvert f_{22}^0\rvert^2$ (mb/sr)	382	5780	43 550
f_{21}^0 (fermi)	$-2.24-1.39i$	$-6.70-3.85i$	$-12.44-6.09i$
f_{22}^0 (fermi)	$0.28+6.18i$	$1.62+23.99i$	$4.63+65.83i$

difficult quantities to predict from the K^+ and K^- data) disappears if the angular dependence of f_{21} is equal to that of f_{22}. All the sets (see Table I) that we have tried bear out this similarity, and all of them show that both the regenerated K_1 and the elastically scattered K_2 have, for a single collision, an angular distribution of the diffraction type. The size of the nucleus is thus the determining parameter for the computation of R, and it is known well enough. The effect of varying f_{22}^0 (which makes σ_T vary proportionally to $\mathrm{Im}f_{22}^0$) is shown in Table III, where the value of R has been computed as a function of δ for three values of σ_{22}: the value expected from the data on charged K's, one-half this value, and twice this value. The effect on R is clearly not too important compared to the dependence of R upon δ.

Table I shows the parameters of the five trial sets that we have used, and the corresponding values for the quantities that have a bearing on the numerical computation of (27). Clearly, if one limits his choice to nuclear radii and cross sections of reasonably acceptable values, the cross sections σ_{22}, σ_{inel}, and σ_T do not show excessive variations. Table II shows how the same quantities are affected by a change in the meson momentum. Since we have a fairly good knowledge of the meson momentum spectrum, we have made a weighted average with respect to the momentum. Table IV gives an idea of how the optical model calculations are affected by the size of the nucleus. The nuclei represented in the table are the ones of significance in this experiment. These computations use the optical model potentials of Set No. 2 of Table I. The quantity b^2 gives the width of the angular distribution [see Formula (21)] and is essentially determined by the size of the nucleus and the wavelength of the incident wave as is common with diffraction-type processes. Figure 3 shows the angular distribution resulting from the multiple scattering given by formula (23) averaged over momentum. The curves are normalized for the same number of incident K_2. For comparison, the dashed line represents the diffraction pattern for a single collision on a nucleus.

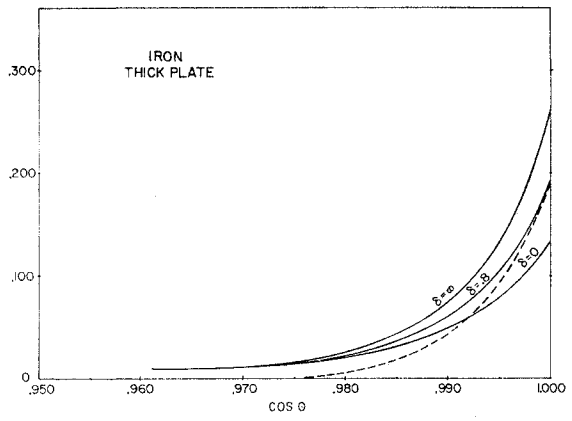

FIG. 3. Angular distribution resulting from multiple scattering, for three values of δ. Momentum of incident K_2 beam is taken from experimental spectrum (Fig. 9). 30.3% have $P=565$ Mev/c, 43.4% have $P=670$ Mev/c, 26.3% have $P=775$ Mev/c. Ordinate: number of events per unit of $\cos\theta$ for one incident K_2. The dashed curve represents the shape of the angular distribution for regeneration at a single nucleus.

SECTION III

Experimental Procedure

Figure 4 shows the experimental arrangement. A circulating beam of protons accelerated by the Bevatron to an energy of 5.3 Bev impinged upon a copper target inside the Bevatron. The target was placed so that 1.1 Bev/c π^-'s emerging in the forward direction were deflected out of the Bevatron through an existing port by the Bevatron's magnetic field. This beam entered a chain of bending and focusing magnets designed to select those particles having a momentum of 1.1 Bev/c $\pm 5\%$ and to pass them through the liquid hydrogen target. This beam is shown schematically in Figs. 5 and 6 with the central trajectory straightened out for clarity, so that only particles which deviate from the central momentum (1.1 Bev/c) show any deflection in the bending magnets.

The first quadrupole L_1 focused the Bevatron target on the second quadrupole L_2. The second quadrupole focused the first quadrupole onto the 60-in. hydrogen target, and the third quadrupole focused the second quadrupole at a point somewhat beyond the propane bubble chamber in order to minimize spreading and possible scattering of the beam after it left the hydrogen target. The first magnet C_1 was adjusted to a small field value in order to maximize the pion beam. The bending magnets H_1 and H_2 counteract the dispersion caused by the Bevatron's magnetic field. All momenta

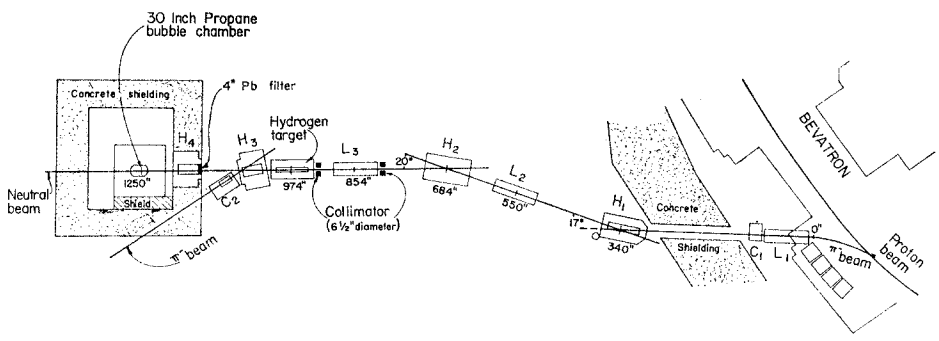

FIG. 4. Layout of the beam (1.1-Bev/c π^-). L_1, L_2, L_3, are 8-in. quadrupole triplets. H_1, H_2, H_3, H_4, and C_2 are bending magnets. C_1 is a correcting magnet.

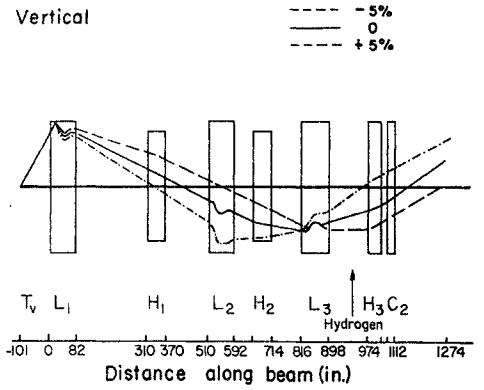

FIG. 5. Pion trajectory (vertical plane). T_V is virtual target in vertical plane.

selected by the system passed through an area about 5 in. in diameter in the hydrogen target.

The reaction $\pi^-+p \rightarrow K^0+\Lambda$ or $K^0+\Sigma^0$ gives rise to a beam of long-lived neutral K_2 particles. The K_2 particles that came off in the forward direction ultimately passed through the 30-in. bubble chamber, modified for this experiment by the inclusion of a metal plate within the propane (see Figs. 7 and 8). The propane bubble chamber has been described by Powell *et al.*[20] After passing through the hydrogen target, the charged beam was swept to one side by the bending magnets H_3 and C_2, and hence was separated from the neutral beam.

The behavior of the pions under the influence of the Bevatron's magnetic field was computed by means of an IBM 650 computer. For subsequent calculations it was possible to replace the relatively complicated Bevatron fringing field and target with a "virtual target." Using an electrical analog computer,[21] trajectories for the pions were calculated from the virtual target through the magnet chain to a point safely beyond the propane bubble chamber. In the design of the beam, particular care was exercised to minimize the amount of the pion beam which would collide with the sides of the magnets, and which would have resulted in contamination of the beam with unwanted charged and neutral particles. The approximate field strength so obtained from the analog computation was refined by wire orbit measurements. When a pion beam was obtained, the current settings received a final adjustment with the aid of electronic counting techniques.

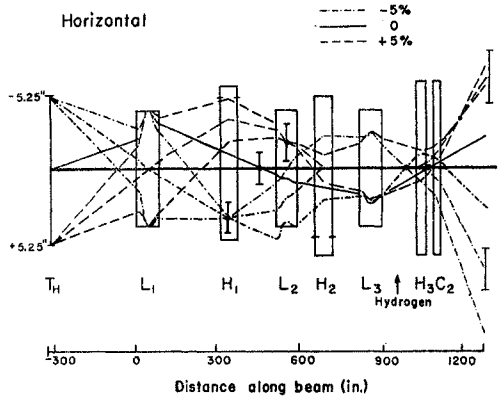

FIG. 6. Pion trajectory (horizontal plane) T_H is virtual target in horizontal plane. The central trajectory is drawn as a straight line.

[20] W. M. Powell, W. B. Fowler, and L. Oswald, Rev. Sci. Instr. 29, 874 (1958).
[21] R. H. Good and O. Piccioni, Rev. Sci. Instr. 31, 1035 (1960).

The chamber was operated at a repetition rate of 12 per minute in a magnetic field of 13.4 kgauss. 206 000 Bevatron pulses were photographed stereoscopically. For the first 123 000 pictures this plate consisted of two parts, one lead and one stainless-steel, each $1\frac{1}{2}$ in. thick, as shown in Fig. 7. For the rest of the pictures, up to 206 000, this plate was replaced with a stainless-steel plate 6 in. thick which was intended to enhance the transmission regeneration effect. Figure 8 shows view 1 of picture 205 216; a K_1 meson decay is visible near the center of the chamber.

The Bevatron beam level was generally between 5×10^{10} and 10^{11} protons per pulse. The total number of protons striking the Bevatron target was

4.8×10^{15} protons, $1\frac{1}{2}$-inch lead and iron plate;

7.2×10^{15} protons, 6-inch iron plate.

These figures were established by monitoring the internal proton beam of the Bevatron; in portions of the experiment in which such monitoring was not complete, values were interpolated by means of counting the frequency of occurrence of certain types of tracks in the bubble chamber.

Scintillation counters were employed to establish the number of negative pions entering the hydrogen target. The number, which includes a correction of approximately 20% due to contamination of the pions with muons (5%) and electrons (15%), is one pion per 6×10^4 protons.

The pions, of momentum 1.1 Bev/c ($\pm5\%$), struck a liquid hydrogen target which was 60-in. long. The regenerating plate of the propane bubble chamber lay 276 in. beyond the center of this target. It was 4 in. high

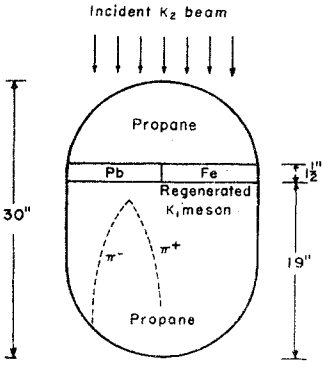

FIG. 7. Schematic drawing of the chamber with the thin plates (top view).

by $14\frac{1}{2}$ in. wide and thus subtended a solid angle of 7.6×10^{-4} steradian. Using the following values,

0.42×10^{23} protons/cm^3 in liquid hydrogen,
0.15 mb/sr for ΛK^0 production,
0.05 mb/sr for ΣK^0 production,
6.5 relativistic solid-angle contraction in laboratory frame,

we find:

$$6.3\times10^{-6}\ K^0 \text{ per pion},$$

which is $0.525\times10^{-10}\ K_2$ per proton (of Bevatron beam).

For the K_2's produced in the hydrogen target, the probabilities of surviving the various hazards are:

0.92 for escaping absorption in the hydrogen target;
0.47 for escaping absorption in the 4-in. lead plate (which filtered out most of the photons present in the beam);
0.95 for going through the collimator;
0.85 for escaping absorption in the 2-in. thick iron frame (surrounding the thin window of the chamber) which covered 65% of the beam cross-sectional area.
0.76 for not decaying before reaching the plate.

This gave a total probability of 0.264 for surviving until the plate in the chamber. Thus we have 1.35 K_2 incident on the plate per 10^{11} protons in the Bevatron beam.

For the study of regeneration (transmission and diffraction) in the plate, the various efficiencies associated with our method of observation are:

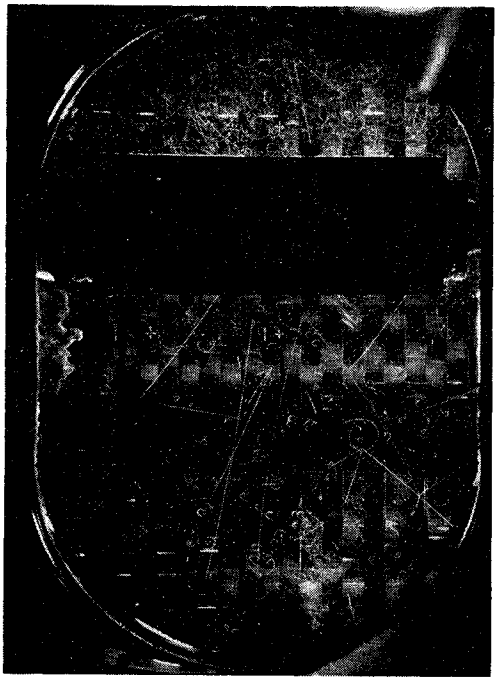

FIG. 8. Decay of K_1 regenerated in the thick plate. $\cos\theta=0.987$, $Q=234$ Mev, $P=809$ Mev/c, $T=0.43$ mean lives.

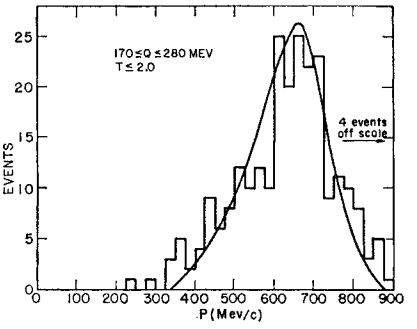

FIG. 9. Momentum distribution of the events having $T\leq2$, $170\leq Q\leq280$ Mev. Curve shows the expected distribution. (See text.)

0.67 probability of charged-mode decay;
0.89 scanning efficiency;
0.70 fraction of events that are measurable;
0.95 fraction of K_1 decays with $170<Q<280$ Mev;
0.90 fraction of events with $P>500$ Mev/c;
0.86 fraction of events with $0<T<2$ K_1 mean lives; and
0.80 fraction of events with π^+ momentum less 600 Mev/c.

The total detection efficiency is thus 0.245. Scattering of K_2's in the 4-inch lead plate, which tends to smear out the transmission peak, has a limited effect due to to the distance (110 in.) between the plate itself and the chamber. Particles scattered at angles larger than $\pm1.5°$ have small probability of reaching the plate in the chamber. No more than a third or so of the particles escaping from the lead filter have suffered nuclear scattering. The two-in. iron frame, which covers 65% of the beam changes the direction of only 10% or less of the K_2 particles.

A pion momentum of 1.1 Bev/c was chosen because at the time of the experiment the cross section for K^0 production appeared to be maximum at this momentum. The pion beam was designed for a momentum range of $\pm5\%$. Although not experimentally verified, the number of pions as a function of momentum is assumed to be a Gaussian centered at 1.1 Bev/c and with a standard deviation of 0.055 Bev/c as determined from the design of the beam. We use this pion distribution to determine the momentum distribution of the regenerated K_1's which have closely the same momentum as their parent K_2's. All parameters that are a function of momentum will affect the shape of this distribution. These parameters include ΛK^0 and ΣK^0 production cross sections, conversion of center-of-mass solid angle to laboratory solid angle, K_2 decay, and our imposed criterion that the π^+ momentum be less than 600 Mev/c. Taking all of these factors into account, the final momentum distribution of K_1's regenerated in the plate and decaying in the chamber is shown in Fig. 9, where it is compared to the experimental momentum distribution.

SECTION IV

Data Analysis

Possible K_1 from the plate must be distinguished from the background of other V-type events which are caused by K_2 and Λ^0 decay and neutron interactions in the propane. Much of the background may be eliminated at the scan table. Fortunately, most of the background V's have an identifiable proton as one of the prongs and therefore these events may be rejected as not being K_1's. However, it was difficult to distinguish protons from positive pions on the basis of ionization at a momentum much above 600 Mev/c; consequently, all events having a positive prong whose momentum exceeded 600 Mev/c were discarded. From the expected K_1 momentum distribution it has been calculated that this criterion will remove 20% of the K_1 mesons. The number of background events removed by this criterion exceeded the number of K_1's removed by a factor on the order of 100 (although most of these background events would have been removed by other criteria).

About 1200 events were thus accepted from about 15 000 events examined. These were measured either on stage microscopes, with digitizers which automatically punched IBM cards, or on an automatic measuring and card punching machine. Either machine measured the position of the origin of an event and points along each track. From these data an IBM 704 computer program spatially reconstructed the event in the chamber and calculated the momentum for each track from its curvature. A subsequent program computed the Q value of the event, assuming that both tracks were pions, and calculated the momentum of the presumed K_1 meson.

Before describing the selection of events used for the study of the regeneration in the plate, it pays to discuss briefly the data concerning all the unselected events. Figure 10 shows the obtained Q distribution. We have, by a numerical calculation (IBM 704), computed the Q distribution expected for events representing three-body K_2 decays, taking into account that electrons or muons originating in such decays have been treated as pions in obtaining the histogram of Fig. 10. This distribution is the curve marked "K_2." The "K_1" curve in the same figure is the Q distribution of K_1 events taken from Fig. 11. The K_1 and K_2 distributions have been mixed in such proportion as to give the best fit to the histogram. With this procedure we ignore, at the moment, the contribution due to nuclear interactions of neutrons or gamma rays because an analysis of the histogram in terms of three distributions cannot be profitably made. The histogram of Fig. 10 is at any rate consistent with the conclusion that most of the events which are not K_1 decays are due to K_2 decays. This simple interpretation would assign 374 events to K_1 decays and 706 to K_2 decays. Knowing that 1.02×10^5 K_2's have crossed the 27 cm of propane, from the mean life of K_2 mesons and the partial decay rates[22] (15.2% in three pions, 41.4% into pion, muon, and neutrino, and 43.4% into pion, electron, and neutrino) we expect to detect 574 K_2 decays. The balance of 132 events is probably due to nuclear interactions, though we must remember that the K_2 flux is only known to $\pm25\%$. Figure 12 shows the Q distribution of such nuclear interactions. We selected events which have two pion tracks

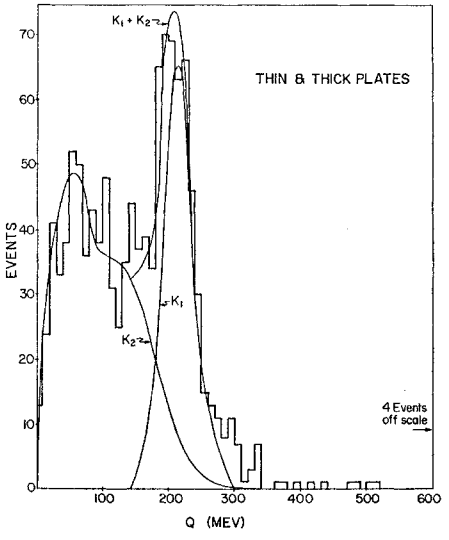

FIG. 10. Q distribution for all events. The computed curve K_2 is the distribution expected from K_2 decays analyzed with the assumption that both charged prongs are pions. Curve K_1 and K_2 is the sum of curve K_2 and a curve proportional to that of Fig. 11. There are 706 events under the K_2 curve and 374 estimated K_1 decays. Although the background seems to be reasonably well accounted for by K_2 decay, some background produced by neutron stars (see Fig. 12) could very well be introduced and still a good fit could be obtained (see text).

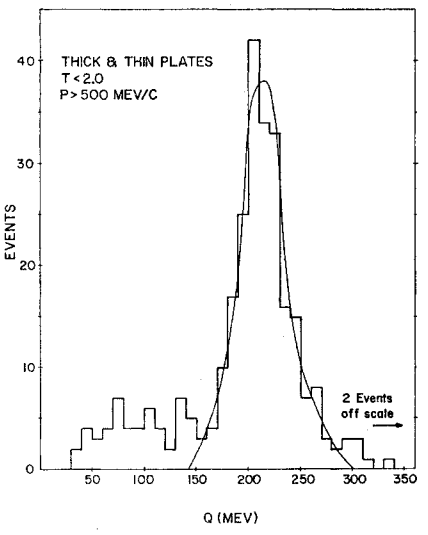

FIG. 11. Q distribution for events with $T\leq2.0$ K_1 mean lives and $P>500$ Mev/c.

[22] S. Okubo, R. E. Marshak, E. C. G. Sudarshan, W. B. Teutsch, and S. Weinberg, Phys. Rev. **112**, 665 (1958); M. Gell-Mann and A. H. Rosenfeld, Ann. Rev. Nuclear Sci. **7**, 407 (1957).

of opposite sign accompanied by a short, heavy prong, in much the same fashion as it was done by Lander[4] in his study of K_2 interactions in propane. This type of event, certainly not due to K_1 or K_2 decay, should have a Q distribution close to that of stars caused by neutrons and gamma rays, that could have been mistaken as decays of neutral K's. These three-prong stars number about 100 in all the pictures. There are probably as many corresponding stars produced by neutral primaries, within a factor of a few units. Clearly, the Q distribution of these events is such that very few of them fall within the interval of 170 to 280 Mev which we have established for K_1 events.

SECTION V

Plate Regeneration

To select events due to regeneration in the plate (by transmission or by diffraction) we use the knowledge that they must satisfy three independent criteria:

(1) The Q value must range between 170 and 280 Mev; this interval is chosen knowing that the measurement errors will cause only 5% of the true K_1 events to be outside the interval.

(2) The time of flight T of the neutral meson, before decay, must be less than two, in units of the K_1 mean life (13.5% of the K_1's live more than two mean lives).

(3) The momentum of the K_1 must be larger than 500 Mev/c. This excludes 10% of the true K_1 decays.

Interactions which are not due to K_1 decay will not, in general, satisfy any of these criteria, and if they happen, by chance, to satisfy two of them, the probability of satisfying the third is not enhanced. A test of the reliability of these criteria for the sample in question can thus be made by selecting pictures which satisfy two criteria and plotting the distribution versus the third variable. This has been done in Figs. 9, 11, and 13, with quite a satisfactory result. After the triple selection in Q, P, and T the residual background must be next to negligible for our purposes.

Using Formulas (23) and (24) and our over-all detection efficiency of 0.245 we estimate, for the total number of 1.668×10^5 K_2 arriving on the three plates, the number of K_1 regenerated in the plate by transmission and diffraction which we should observe to

TABLE V. Total numbers of K_2's and of regenerated K_1's which satisfy the acceptance criteria.

	1½-in. lead	1½-in. iron	6-in. iron
K_2's incident on plate	0.333×10^5	0.333×10^5	1.00×10^5
Estimated K_1's per K_2	0.00296	0.00468	0.00436
K_1 expected (including 24.5% detection eff.) according to Set No. 2 of Table I	24.2	38	107
K_1 found experimentally	26	41	92

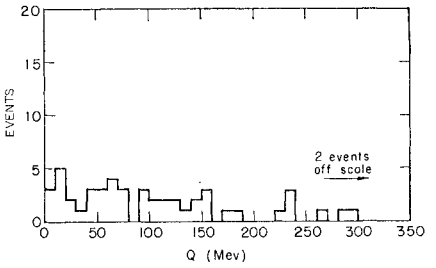

FIG. 12. Q distribution for 3-prong events (see text).

decay. Table V gives the comparison with the experimental results.

The error in the number of K_2's is probably some 25%. Table I shows that, according to which set of interaction parameters we use, the regeneration cross section σ_{21} varies from 8.6 to 25 mb. Sets No. 2 and No. 5 seem to be preferred, but due to the imprecise knowledge of the K_2 flux and also of the optical model parameters, this result cannot be construed as being conclusive. Set No. 5 was included in Table I because earlier experiments on K^- mesons appear to show $\sigma_{\text{tot}}=55$ mb when interpolated to our K_2 energy. Recent experiments[15] now give $\sigma_{\text{tot}}=33$ mb.

The angular distributions of the selected events are shown in Figs. 14–16 for the thick plate and for the lead and iron parts of the thin plate. The curves show the angular distribution expected from the diffraction and transmission regeneration. The agreement between the theoretical curves and the experimental histograms is quite satisfactory. The presence of the transmission peak is clearly shown by the difference between the angular distribution near the plate (Fig. 17) where a

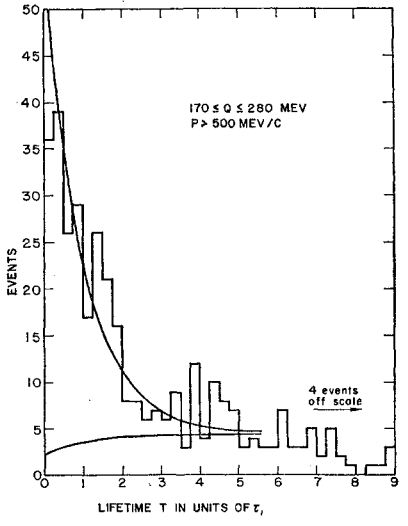

FIG. 13. Lifetime distribution of events with Q and P in the accepted range, measured in K_1 decay lengths. The lower curve represents the estimated background. The upper curve is the K_1 decay exponential plus the background of the lower curve. Notice that the background drops off beyond $T=7$ due to the finite length of the chamber.

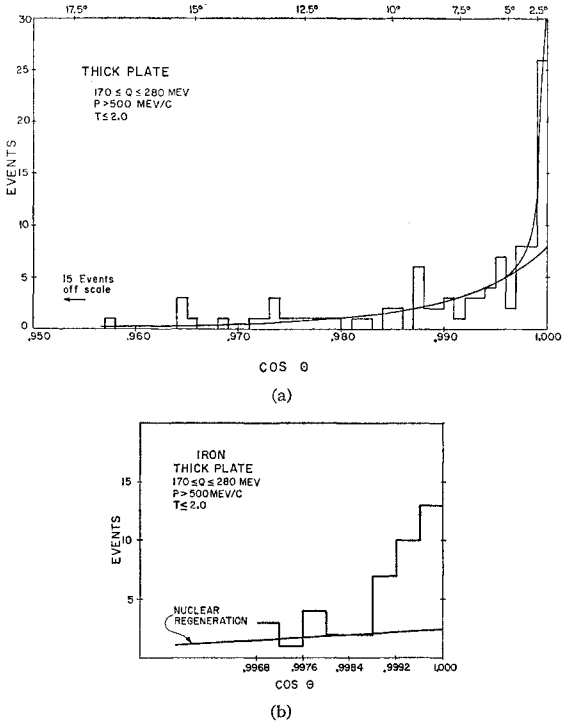

FIG. 14. (a) Angular distribution of events from the 6-in. iron plate. The upper curve is the Gaussian $\exp(-\theta^2/2w^2)$ with $w=2.2$ degrees. The lower curve shows the distribution expected from multiple scattering, excluding transmission regeneration. (b) Angular distribution for the thick plate on expanded scale showing the structure of the transmission peak.

peak is expected, and far from the plate (Fig. 18) where no peak should be observed. Also, comparison between Fig. 17, related to K_1's regenerated by iron nuclei, and Fig. 22, related to K_1's regenerated by nucleons, gives strong evidence for the diffraction-regeneration phenomenon.

Because of the limited number of events, we have chosen to derive quantitative conclusions only from graphs where the events are grouped in 0.001 intervals for $\cos\theta$, as in Figs. 14–18. However, some information can be derived from the graph of Fig. 14(b) where the events are grouped in 0.0004 intervals. We see that the maximum still seems to occur for the interval closest to the forward direction, which includes particles regenerated within 1.6 deg from the forward direction.

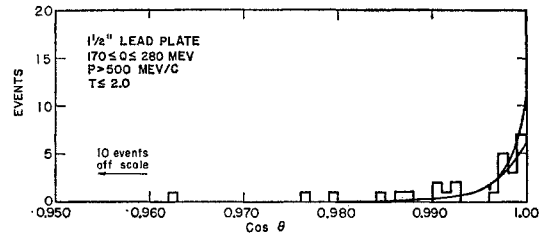

FIG. 15. Same as Fig. 14(a), for the $1\frac{1}{2}$-in. lead plate.

The expanded graph also gives an indication that the peak, as observed with our apparatus, has a distribution closely represented by $\exp(-\theta^2/2w^2)d(\cos\theta)$ with $w=2.2$ deg. An approximate computation of the angular resolution showed that we could expect w to be as large as 3 deg. On the other hand, no imaginable instrumental error could sharpen the observed peak. For instance, the detection efficiency could not possibly be larger for K_1's at angles less than two degrees than for much wider angles.

We thus conclude that the transmission peak is as sharp as could be expected and it has the expected shape. It is also of some value to note that a peak is observed in both the thick and the thin iron plate data.

Let us now estimate the probability that the peak is due to statistical fluctuation.

For that purpose we compare the number of events in the two $\cos\theta$ intervals, 0.970 to 0.997 and 0.999 to 1. Adding up the thin and thick plate, we find 73 events in the large interval. Our computed angular distribution shows 12 ± 1.4 events should be found in the small interval if δ were larger than, say, 5.

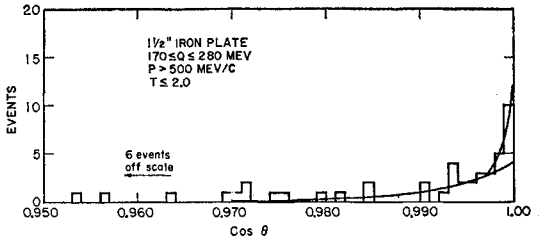

FIG. 16. Same as Fig. 14(a), for the $1\frac{1}{2}$-in. iron plate.

With the Poisson distribution we then compute that, in the absence of a real cause for a forward peak, only one in three million experiments such as ours would show 36 or more events in the $\cos\theta$ interval between 0.999 and 1. The probability that the mass difference is higher than five, for which value no possible choice of nuclear parameter would give a discernible transmission peak, is thus of the order of 10^{-6}. In a similar fashion, we compute that for $\delta=1.2\ \hbar/\tau_1$ we should observe 17.6 ± 2.7 events in the 0.999 to 1.000 interval for the thick iron plate only. The probability of observing 26 or more instead of 17.6 is then 5%, so that with such a confidence level we can say that δ is less than $1.2\ \hbar/\tau_1$.

Actually not all of the transmission component is included in the first interval. In computing the upper limit for δ as we have just done, this is by far not as important as selecting a range where the transmission component represents a large fraction of all the events, but when computing the most probable value and the lower limit for δ the best procedure is to consider the three intervals closest to the forward direction. This angular range, as Fig. 14(a) and (b) show, includes practically all the transmission component. The useful quantity to be calculated is therefore the ratio S of the

intensity in the solid angle represented by the interval $\cos\theta=1.00$ to 0.997, to the intensity in the interval $0.970<\cos\theta<0.997$.

Figure 19 shows this theoretical curve as a function of δ. The same remarks made in Sec. I.C about the quantity R apply to S as well. The curve has been computed for different values of nuclear parameters (Table I); they all yield substantially the same result.

The experiment gave 42 events between $0.997<\cos\theta<1$ and 50 events in the range $0.970<\cos\theta<0.997$. The experimental value for the ratio S is therefore 0.82 ± 0.18. From Figs. 14 and 19 we thus obtain that the mass difference δ is $0.92_{-0.20}^{+0.30}$. Perhaps a better value for δ is obtained by subtracting from the events appearing in the first 8 cm from the plate, a proportion of the number of events observed at more than 8 cm from the plate. We know that this zone must contain $e^{-2}=13.5\%$ of the number of events (92) observed in the zone near the plate ($T=0$ to $T=2$). After subtracting this known amount, the rest is considered background. Since there is no propane in the plate, the propane regenerated K_1's are not as numerous in the first zone as they are in the second. We take this fact into account by multiplying the background (only in part due to K_1's) by a factor of 0.8. We thus subtract $0.8(2.79)=2.23$ events from the interval $0.997<\cos\theta<1$ and $0.8(6.58)=5.26$ from the interval $0.970<\cos\theta<0.997$. We obtain 39.77 and 44.74 K_1 events in the two intervals, which gives $S=0.89\pm0.21$ and $\delta=0.84_{-0.22}^{+0.29}$.

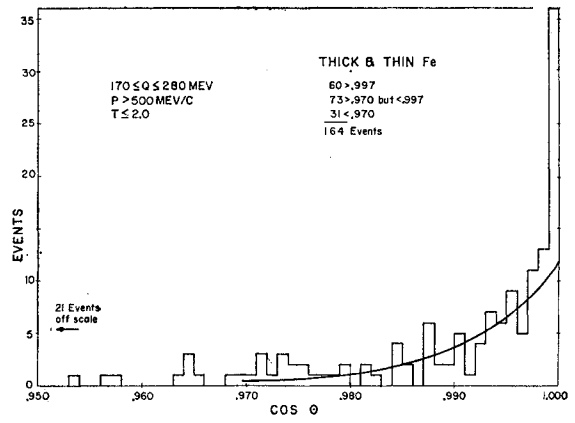

FIG. 17. Angular distribution of all events that originate in either the 6-in. or the $1\frac{1}{2}$-in. iron plate and that satisfy the criteria $170\leq Q\leq 280$ Mev, $P>500$ Mev/c, and $T\leq 2.0$ mean lives.

Let us now express quantitatively the confidence that δ is larger than zero. The value of S corresponding to $\delta=0$ is 1.57, that is 2.92 standard deviations from the experimental value 0.928 ± 0.220. This gives a probability of 2 in a thousand. With a similar computation we find that with a probability of 5% δ can be less than $0.44\ \hbar/\tau_1$.

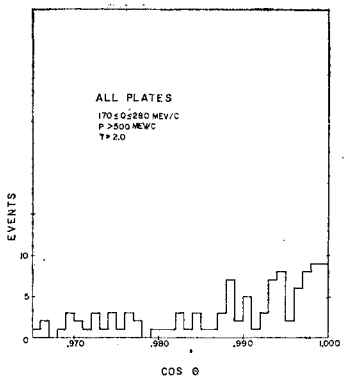

FIG. 18. Angular distribution of all events that satisfy the criteria $170\leq Q\leq 280$ Mev, $P>500$ Mev/c, and $T>2$ mean lives.

The above value of δ has been obtained from the 6-in. iron plate angular distribution data since a plate of this thickness provides the most sensitive test of the mass difference. Using the value $\delta=0.84$ and the observed number of K_1's for the thick plate, we can now compute the absolute number of K_1's expected from the thin iron and lead plates. This prediction for the iron plate should even be independent of our computed σ_{21}. Only the ratios of our beam monitoring should contribute a systematic error. We thus expect 38 and 24.2 events for iron and lead, respectively, and we find 41 and 26.

Inspection of Fig. 16 shows that a transmission component is also present for the thin plate. Indeed, for $\delta=0.08$, the $1\frac{1}{2}$-in. iron plate should have $S=0.87$ (Fig. 20). The data give $S=17.8/19.3=0.92\pm0.3$, which is in reasonably good agreement, thereby supplying additional evidence for the existence of a transmission peak.

For the $1\frac{1}{2}$-in. lead plate the diffraction regeneration is at smaller angles than for iron; thus it invades the angular range of the transmission component. For this reason, the value of δ obtained from the lead data has

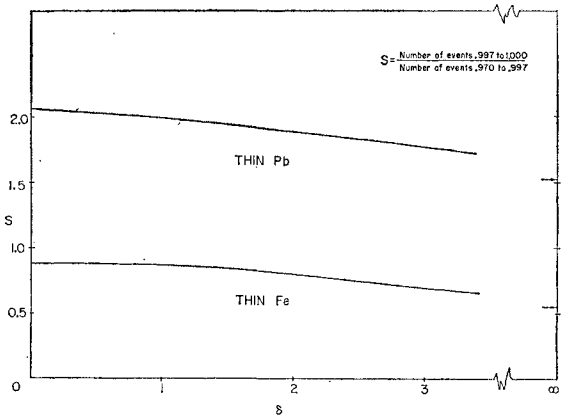

FIG. 19. Calculated ratio S of numbers of events of the two $\cos\theta$ intervals 1 to 0.997 and 0.997 to 0.97 as a function of δ. The quantity $(S-0.5)$ is approximately proportional to the transmission regeneration. Experimental value for S is 0.89 ± 0.21.

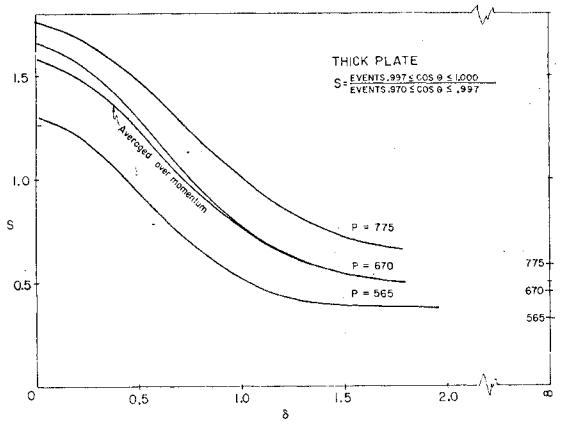

FIG. 20. Same as Fig. 19 for the 1½-in. Fe and 1½-in. Pb plates. Experimental values were 0.92±0.3 for Fe and 2.03±0.8 Pb.

less *a priori* significance than that from the thin iron plate. The expected value of S for lead is 2.02 (Fig. 20), and the data give $14.8/7.3=2.03\pm0.8$.

SECTION VI

Propane Regeneration

Using the value of σ_{21} of 8.3 mb, Table III, and assuming that 10^5 K_2's traversed the propane in the course of the experiment, we have calculated that there should have been about 80 K_1's that were regenerated due to carbon diffraction. Presence of this number of K_1's, while consistent with the data, is not demonstrable because of the large background (about 600 events), which presumably consisted mainly of K_2 decays and neutron stars.

A search for decay events associated with an interaction which could have been the origin where a K_1 was regenerated by a K_2 collision with a proton, free or bound, yielded 20 examples with a good fit to the kinematics for K_1 regeneration at that origin. The distribution of the time of flight for these events (Fig. 21) follows quite satisfactorily the expected mean life (solid curve). The angular distribution of these K_1's (Fig. 22) is much broader than the distributions for the plate-regenerated K_1's (Figs. 14–16) confirming that a nucleonic regeneration is responsible for the K_1's with origins, while a coherent regeneration produces K_1's decaying near the plate. The twenty events indicate a cross section of about 0.5 mb for regeneration by protons.

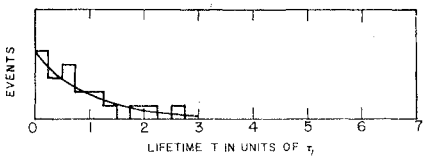

FIG. 21. Lifetime distribution of K_1 decays with origin. These K_1's were regenerated in collisions with individual nucleons.

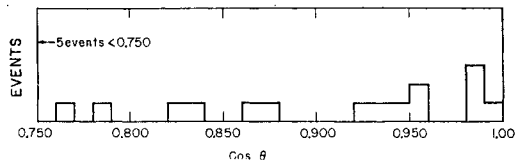

FIG. 22. Angular distribution of the K_1's regenerated in K_2-nucleon collisions. Note the large angular spread compared to Figs. 14(a) and 17.

SECTION VII

Conclusion

The Q distribution of Fig. 10 proves the reality of the K_2-K_1 regeneration. To our knowledge, this is the first time that this phenomenon has been observed. Moreover, the angular distribution of the regenerated K_1 constitutes convincing evidence that the expected diffraction regeneration by the nuclei of iron and the transmission regeneration by the plate do indeed occur. The peak in the angular distribution, showing that K_1 particles are produced by K_2's within two or three degrees of the direction of the primary particle, can hardly be imagined to be produced by an instrumental error. The mere existence of such an unusual type of particle production gives strong reassurance that the particle mixture theory is correct, and that the mass difference between K_1 and K_2 is no more than a very few units. Quantitatively, the mass difference deduced from the experiment is $(0.84\pm0.25)\hbar/\tau_1$, that is, 5.5 ± 1.7 μev. With 90% probability, δ is between 0.44 and 1.2 $\hbar/\tau$. The error quoted is only the statistical uncertainty. The errors produced by the necessity of using, in the computation, parameters that could only be estimated, is probably less than the statistical uncertainty.

The measured mass difference is 10^{-14} times the mass of the K meson. The detection of such a minute fractional difference is directly connected with the fact that the production of undeflected K_1's takes place not in a single nucleus, but in a large number of nuclei through the whole depth of the plate. It is actually interesting to note another consequence of this production mechanism; the spread of the mass spectrum of the produced K_1's is less (about one-half) than the spread for K_1 mesons produced in interactions with single nuclei. This is due to the fact that the K_1 amplitude of the transmission wave extends for the whole depth of the plate, which is four decay lengths. This sharpening effect, which becomes more pronounced with thickening of the plate, would make possible the measurement of a mass difference substantially smaller than the "natural" mass spread of the short-lived K_1. For contrast, if the mass difference were of several units the intensity of the transmission component would rapidly drop to negligible values, as a consequence of the practically complete incoherence of the K_1 and K_2 waves inside the plate.

As Okun' and Pontecorvo[23] pointed out, the rate of transition between the K^0 and $\bar{K}^0$ states, which is proportional to the mass difference between K_1 and K_2 because this difference governs the speed at which the K_1 and K_2 states go out of phase with respect to each other, is also proportional to the first power of the coupling constant for a strangeness change of two units. In the decay of a particle of strangeness two into a particle of strangeness zero, the rate is proportional to the square of the same coupling constant. Therefore, the finding that the mass difference is of the order of $\hbar/\tau_1$ implies that the transition of K^0 and $\bar{K}^0$ takes place in about 10^{-10} sec, while the decay of the Ξ into a proton and a meson will have a mean life of 10^{-5} sec. Obviously it would be very difficult to set such a limit by direct means.[24]

We cannot compare our experimental value for δ with any theoretical calculation. After the brief remark by Gell-Mann and Pais that the different lifetimes of K_1, K_2, requiring different widths for the two mass spectra, also imply a mass difference for the two particles, nothing has been added on this subject.[25] It may, perhaps, be looked on with satisfaction that the mass difference is indeed, within a factor less than two, equal to the mass width. This may indicate that the mass differences produced by the weak interactions are in the domain where theoretical guesses are true.

ACKNOWLEDGMENTS

We are grateful to many people who generously contributed to this experiment, particularly Edward J. Lofgren, Myron L. Good, Richard L. Lander, Robert E. Lanou, Marian N. Whitehead, Roy Kerth, Frank T. Solmitz, Warner Hirsch, and Karl Brunstein. Larry Oswald and many other members of the Bubble Chamber Group ably assisted during the Bevatron run. The pictures were scanned by Mrs. Glennette Armeson, Vic Dahmen, Mrs. Roksalana Gamow, Layton Lynch, and Mrs. Ottilie Oldenbusch.

[23] L. Okun' and B. Pontecorvo, J. Exptl. Theoret. Phys. (U.S.S.R.) **32**, 1587 (1957) [translation: Soviet Phys.—JETP **5**, 1297 (1957)].

[24] After this manuscript was completed, a paper by S. L. Glashow appeared in Phys. Rev. Letters **6**, 196 (1961), where it is noted that the remark by Okun' and Pontecorvo only applies to the C-even part of the interaction responsible for the decay of the Ξ.

[25] The sign of the mass difference (whichever of K_1 or K_2 is the heavier particle) remains, of course, unknown. Again, no theoretical indication is available. Experiments to detect the sign of δ have been suggested by J. Sandweiss (private communication); N. Biswas, Phys. Rev. **118**, 866 (1960); and I. Yu. Kobzarev and L. B. Okun', J. Exptl. Theoret. Phys. (U.S.S.R.) **39**, 605 (1960) [translation Soviet Phys.—JETP **12**, 426 (1961)]. Another interesting phenomenon connected with the neutral K meson is its possible electromagnetic interaction with electrons, treated by Ya. B. Zel'dovitch, J. Exptl. Theoret. Phys. (U.S.S.R.) **36**, 1381 (1959) [translation: Soviet Phys.—JETP **36(9)**, 984 (1959)] and G. Feinberg, Phys. Rev. **109**, 1381 (1958).

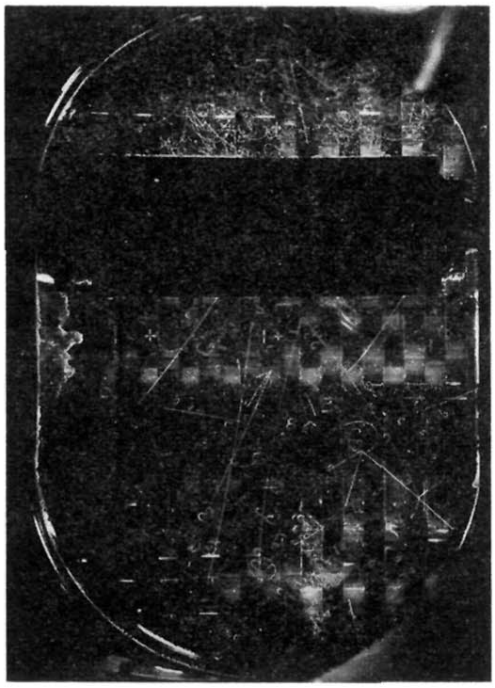

FIG. 8. Decay of K_1 regenerated in the thick plate. $\cos\theta = 0.987$, $Q = 234$ Mev, $P = 809$ Mev/c, $T = 0.43$ mean lives.